# Tuning of the nucleation field in nanowires with perpendicular magnetic anisotropy

Judith Kimling[1], Theo Gerhardt[1], André Kobs[1], Andreas Vogel[1], Sebastian Wintz[2], Mi-Young Im[3], Peter Fischer[3], Hans Peter Oepen[1], Ulrich Merkt[1], and Guido Meier[1]

[1] Institut für Angewandte Physik und Zentrum für Mikrostrukturforschung Hamburg, Universität Hamburg, Jungiusstr. 11, 20355 Hamburg, Germany
[2] Institut für Ionenstrahlphysik und Materialforschung, Helmholtz-Zentrum Dresden-Rossendorf, 01314 Dresden, Germany
[3] Center for X-ray Optics, Lawrence Berkeley National Laboratory, Berkeley, California 94720, USA

## INTRODUCTION

Magnetization reversal in ferromagnetic nanowires is governed by three processes: domain nucleation, domain-wall motion, and pinning. If the nucleation field exceeds any propagation or depinning field, no domain walls can be statically observed. Thus, the nucleation field determines the minimum potential depth of pinning sites to reliably trap domain walls. Weak pinning sites and therefore small nucleation fields are of interest in connection with current-driven depinning of domain walls, since high current densities, which are otherwise required, can modify or even destroy a sample.[1] It was experimentally found that the critical current density for magnetization reversal in systems with perpendicular magnetic anisotropy can be orders of magnitude smaller than in soft-magnetic materials.[2] The high efficiency of the underlying non-adiabatic spin-transfer torque arises from relatively narrow domain-wall widths.[3,4] In nanowires with perpendicular anisotropy, a reduced inversion symmetry can significantly support the magnetization reversal via spin-orbit torque[5] and a recently discovered spin Hall effect based phenomenon.[6] Another advantage of systems with perpendicular anisotropy is that generally Bloch walls appear,[2] whereas in soft-magnetic wires complex two-dimensional spin structures with intrinsic degrees of freedom occur.[7,8] All in all, wires with perpendicular anisotropy, in particular Co/Pt wires, are promising candidates for possible applications based on the displacement of domain walls by spin-polarized currents like in the race-track memory[9] as demonstrated in various studies (see, e.g., Refs. 10,11,12). Furthermore, Co/Pt layered structures are preferably used to investigate domain-wall resistance.[13,14,15] Recently, a new kind of effect, i.e., the anisotropic interface magnetoresistance, was found in these materials.[16,17,18]
In the case of soft-magnetic wires, for example, patterned from permalloy ($Ni_{80}Fe_{20}$), a common strategy to control domain nucleation for studying field- and current-induced domain-wall dynamics is the usage of laterally extended pads of continuous film attached to one of the wire ends. The magnetization reversal commences in this so-called nucleation pad due to its smaller shape anisotropy compared to the wire region.[19] A domain wall is injected from the pad into the wire and propagates until it pins at a defect or at an intentionally created pinning site, for example, a notch[20] or a magnetically softened region.[21] For wires with triangular-pointed ends, the formation of flux-closure domains is suppressed. This leads to an increase of the switching fields compared to wires with flat ends[22,23] or nucleation pads.

In wires with perpendicular anisotropy, nucleation pads do not work as for in-plane magnetized samples since demagnetizing effects play only a minor role. In systems with few defects acting as nucleation sites, the size of the pad has to be in the order of several 100 $\mu$m to observe any effect.[24,25] Nevertheless, smaller nucleation pads were recently used for perpendicularly magnetized wires. Since no systematic studies on the pad design were made, and the samples were usually studied by methods based on transport measurements providing only little spatial resolution such as extraordinary Hall effect[10] or giant magnetoresistance,[26] a proof of concept is still missing. A well known route to decrease

the nucleation field is lowering the perpendicular anisotropy or inducing defects acting as nucleation sites by means of local ion irradiation.[27] For instance, Alvarez et al. demonstrated the functionality of $Ga^+$-irradiated nucleation pads by imaging the magnetization reversal of Co/Pt multilayer wires with a Kerr microscope.[28] Another approach for the nucleation of domains in wires with perpendicular anisotropy is to exploit the Oersted field that accompanies a current pulse flowing through a strip line attached to the wire.[29]

In this study, we demonstrate that in contrast to in-plane magnetized wires, where triangular-pointed ends suppress the nucleation of domains, the nucleation field in Co/Pt wires with perpendicular anisotropy can be decreased by almost 60% by designing tip-shaped wire ends. It is further shown that the nucleation field can be intentionally tuned by varying the opening angle of the tip. Details about sample preparation and magnetic imaging are given in Section 2. Section 3 presents the experimental results and addresses aspects concerning the creation of pinning sites. The experimental results are further discussed in Section 4 along with supporting micromagnetic simulations. Section 5 concludes our study.

## METHODS

Samples were prepared by electron-beam lithography, sputter deposition of the Co/Pt multilayer, and lift-off processing of the resist as illustrated in Fig. 1a. As substrate a silicon-nitride membrane with a thickness of 150 nm was used.[30] The resist[31] was spin-coated with 8000 rpm, baked out at 170 ∘C for 30 min, and exposed with a scanning electron microscope at 10 kV. After development, the sample was treated by reactive-ion etching to remove residuals of the resist in the exposed areas. Then, the thin-film stack Pt(5.0 nm)/[Co(0.7 nm)/Pt(2.0 nm)]×4 was deposited at room temperature at a base pressure below $2 \times 10^{-9}$ mbar: First, a 4 nm thick Pt seed layer was grown via ion-beam sputtering utilizing an electron cyclotron resonance source. Subsequently, dc magnetron sputtering was employed to deposit both a 1 nm thick Pt layer and right afterwards the Co/Pt multilayer.[32] The lift-off was done by dissolving the resist in acetone. In a last step, the sample was rinsed with isopropanol and blow-dried with nitrogen.

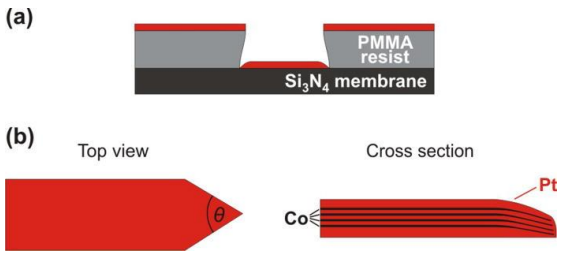


FIG.1
(a) Illustration of sample preparation. (b) Wire geometry: due to shadowing by the resist mask during sputter deposition of the metal film, less material is deposited at the triangular-pointed wire end with tip-opening angle θ.

Magnetization reversal was imaged by transmission soft x-ray microscopy at the XM-1 full field microscope at beamline 6.1.2 of the Advanced Light Source in Berkeley, CA, USA.[33] The setup allows for the application of a magnetic field perpendicular to the sample plane. Magnetic contrast is based on the x-ray magnetic circular dichroism (XMCD) effect.[34] It is proportional to the magnetization components along the projection of the x-ray beam. The perpendicularly magnetized sample was inserted into the microscope setup such that the surface normal was in parallel to the beam direction.

Micromagnetic simulations were performed with the MicroMagnum code.[35] The external magnetic field was applied at an angle of 3° to the surface normal. This symmetry breaking is required to enable domain nucleation since our simulations were performed for zero temperature and other fluctuations are neglected. In case fluctuations and imperfections are not considered, there is usually an offset between the simulated values for the critical fields and the experimental results. This effect is known as Brown's paradox.[36,37] The thickness of the simulated wires was 0.7 nm according to the thickness of one Co layer in the actual sample, and the multilayer structure of the Co/Pt film was not taken into account. Discretization was done using finite differences.

## EXPERIMENTAL RESULTS

Figure 2a depicts a transmission x-ray micrograph of a Co/Pt wire with a triangular-pointed end located at its top, a straight segment with a notch, and a nucleation pad at its bottom end which is not completely visible. The structure was saturated by applying a field of about −200 mT before increasing the reverse field in steps of +0.1 mT. Figures 2b through 2d are differential images revealing the magnetization change between two field steps. Magnetization reversal does not start in the nucleation pad but at the upper end of the wire at an applied field of +11.8 mT, i.e., the nucleation field. More precisely, the reversal process commences with the nucleation of an oppositely oriented domain within the triangular-pointed end. A domain wall propagating top-down is pinned twice before the entire magnetization is reversed at +12.1 mT. The presence of the notch (see arrow in Fig. 2a) has no influence on the mobility of the domain wall.

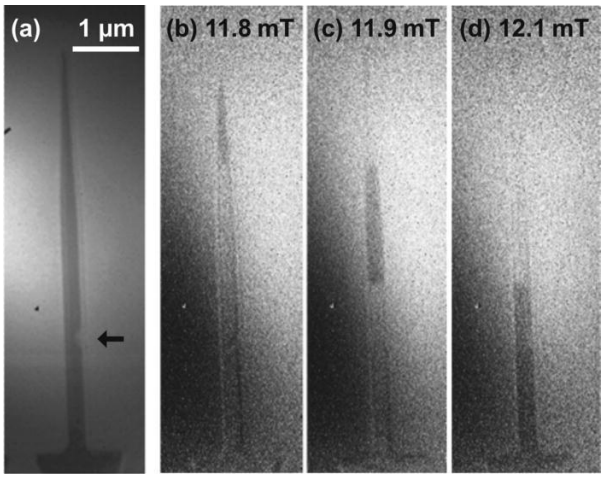


FIG.2

(a) Transmission x-ray micrograph and (b) through (d) corresponding differential images (the respective previous image serves as reference) of a Pt(5.0 nm)/[Co(0.7 nm)/Pt(2.0 nm)]×4 wire with a nucleation pad (bottom, not completely visible), a notch marked by the arrow in (a), and a triangular-pointed end (top) recorded at the given field values after saturation at −200 mT.

We attribute the observed nucleation behavior to a variation of the local anisotropy constant due to shadowing effects during multilayer growth. The Co/Pt multilayer was sputter-deposited onto the resist mask (≈160 nm thick) created by electron-beam lithography. Since for magnetron sputtering the diameter of the source is comparable to its distance to the sample, shadowing by the sample morphology has to be taken into account. In case of the bottom-up approach used, the amount of deposited material locally varies and depends on the lateral distance to the edges of the resist mask. In particular, at the triangular-pointed end, less material reaches the substrate compared to the straight wire segment. The same holds true for geometrical constrictions such as notches. A schematic representation of a straight wire with a triangular-pointed end is shown in Fig. 1b. The left hand side of

the figure depicts the lateral geometry, while the wire's cross-section is sketched on the right. Since Co and Pt are deposited at the same angle towards the sample surface and from the same distance under the same conditions, the ratio of Co and Pt thicknesses in the multilayer stack is unaffected by the reduction of film thickness towards the triangular-pointed wire end. It can be assumed that the saturation magnetization $M_s$ remains basically constant down to very thin layer thicknesses.[38,39] What is left as a changing property is the magnetocrystalline anisotropy constant $K_1 = K_{1,eff} + \mu_0 M s 2/2$ which for the present system mainly originates from interface contributions. We consider a continuous reduction of the anisotropy constant $K_1$ towards the triangular-pointed end of a tip, as well as in other regions where less material is deposited, to be the origin for the reduction of the nucleation field.[40] There are two reasons for the reduction of the anisotropy of the Co/Pt multilayer due to shadowing effects. The first reason is the gradual reduction of the thickness of the Co layer as below $t_{Co} \lesssim 0.5$ nm the first order anisotropy constant $K_{1,eff}$ decreases with decreasing $t_{Co}$.[41] This behavior is in accordance with other studies, see, e.g., Refs. 42,43. The second reason for the gradual reduction of the anisotropy constant is connected with the thickness of the Pt interlayer. When it falls below $t_{Pt} \approx 2$ nm, we observe a decrease of the anisotropy for our multilayer system.[32] This is in agreement with previous results.[44,45] Consequently, a gradual reduction in perpendicular magnetic anisotropy occurs in the regions where the Co- and Pt-layer thicknesses are gradually reduced due to shadowing effects. As discussed in Section 4 it is confirmed by micromagnetic simulations that the reduction of the nucleation field for wires with triangular-pointed ends can indeed be caused by such a reduced anisotropy.

Shadowing effects not only change the anisotropy but also induce defects. Thus, they do not only affect domain nucleation but also the pinning of domain walls. We observe that in wires with periodic lateral modulations domain walls get pinned both at the transitions from wide to narrow and from narrow to wide regions (not shown). Here, the mechanism responsible for pinning is presumably not an increase in domain-wall energy when entering a wider segment, but connected with defects and gradients of the anisotropy in the multilayer due to variations in the layer thicknesses caused by shadowing of the resist mask. Consequently, it has to be cross-checked whether lateral geometrical variations, such as notches or anti-notches, or above mentioned effects caused by shadowing are responsible for pinning. In the latter case, the preparation has to be performed with particular care. The aspect of domain-wall pinning remains a major issue in the field of perpendicularly magnetized media, which shall not be addressed further in this paper, where the focus lies on the nucleation of domain walls.

The dependence of the nucleation field on the wire geometry was studied in detail for three different widths of nanowires, namely, 320 nm, 430 nm, and 570 nm. For increasing tip-opening angles, the total length of a wire decreases from 28 $\mu$m to 20 $\mu$m. The reason for this is that the volume of the wires was kept constant for the different geometries in order to exclude a variation of the switching fields due to a change of the number of volume defects.[46,47] Figure 3a exemplarily depicts scanning electron micrographs of wire ends with different tip-opening angles. Switching fields were determined by transmission x-ray microscopy. After saturation at an out-of-plane field of about −200 mT, a reverse field was applied and increased in steps of +1.1 mT. In the field of view of the microscope, which has a diameter of 10 $\mu$m, about half of the total length of the wires could be imaged. Pinning of domain walls was never observed. Thus, it can be assumed that nucleation field and switching field are the same or close within the uncertainty of a field step of 1.1 mT.

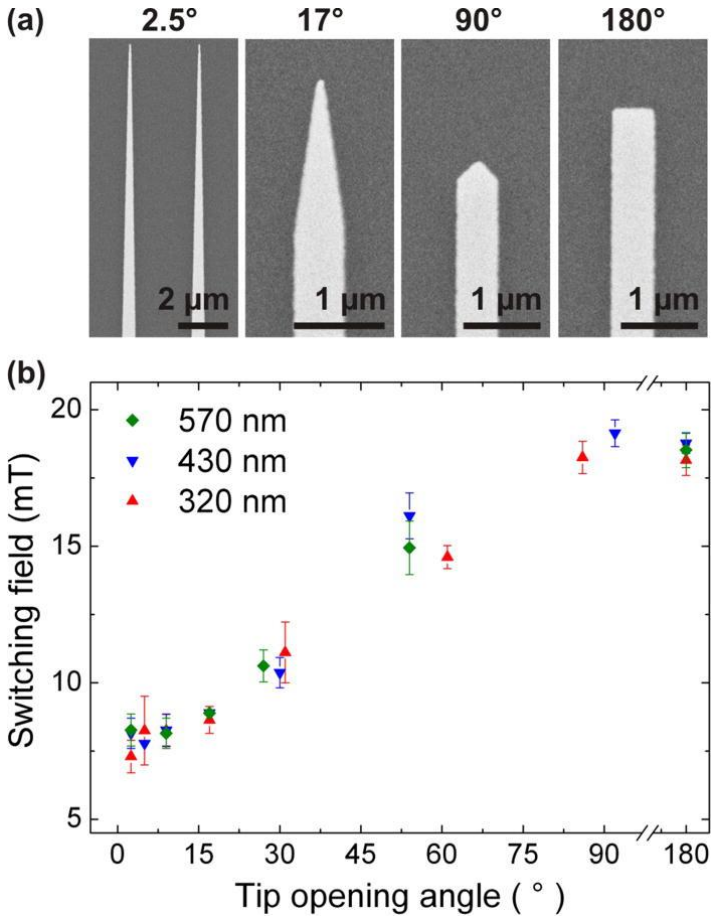


FIG.3

(a) Scanning electron micrographs of wires with various opening angles of the tip's end. (b) Switching field versus tip-opening angle determined by transmission x-ray microscopy for three different widths of nanowires.

Figure 3b depicts the average switching field as a function of the tip-opening angle θ determined from nine field sweeps for each data point. For all three wire widths, the same behavior is observed. The switching fields of wires with a flat end scatter around $(+18.5 \pm 0.5)$ mT. For decreasing angle θ, the switching field decreases to a value of $(+7.9 \pm 0.6)$ mT for $\theta = 2.5°$. This corresponds to a reduction of the nucleation field by $(57 \pm 5)$%. The fact that there is no influence of the wire width on the switching field indicates that nucleation takes place in a volume of the tip end that is provided independently of the tip's length, which increases with increasing width of the wires. That the nucleation takes place in the tip area is in complete agreement with the XMCD images presented in Fig. 2. As stated above, the reduction of the nucleation field is assumed to originate from a decrease of the local anisotropy constant in the tip area due to shadowing during sputter deposition of the multilayer.

Before presenting the results of micromagnetic simulations that support this hypothesis, the impact of the experimental results shall be discussed. The possibility to reliably control the nucleation field shows that the bottom-up microfabrication approach used is worth being pursued. One further advantage of this preparation method is that it is based on a single lithography step. This distinguishes it from other methods that require a second preparation step to diminish the nucleation field, for example, local ion irradiation. A possible disadvantage of the bottom-up approach used is that shadowing effects do not only cause a modulation of the multilayer stack along the axis of a wire due to triangular-pointed ends.

At all edges of a wire, the multilayer does not end abruptly but the thickness gradually decreases on the way to the edge according to the scheme of Fig. 1a. The alternative patterning approach is to deposit the magnetic film first, to employ lithography with a negative resist, and to pattern the nanowires top-down by etching. Besides the disadvantage of more steps of sample preparation in the top-down approach, also the problem of edge damage cannot be excluded with this method. It has been shown by Shaw et al. that even small variations in the edge properties can completely change the reversal behavior of perpendicularly magnetized nanostructures.[48] Furthermore, possible damage of the entire multilayer system[24] can occur during etching if the film is only protected by a resist mask and not, for example, by a titanium layer.[25] Anyway, with the bottom-up approach pursued in this work we can be sure that the multilayer stack is not significantly modified in the center of the wires compared to the pristine film, which can be concluded from the fact that rectangular wires with flat wire ends of arbitrary width exhibit the same switching field.

## MICROMAGNETIC SIMULATIONS

To study the influence of both the anisotropy variation and the tip geometry on the switching field, micromagnetic simulations were performed. The width of the wires in the simulations was taken as 320 nm in accordance with one type of wires studied in the experiment. The local anisotropy constant was reduced linearly in the tip area from the maximum value $K_1$ to $K' = a \cdot K_1$ at the very end as sketched on the right hand side of Fig. 4a. The total reduction of the local anisotropy constant was varied between zero ($a = 1.0$, $K1,eff' = 350\,kJ/m^3$) and 20% ($a = 0.8$, $K1,eff' = 34\,kJ/m^3$). At an anisotropy reduction of $a = 0.78$, the spin-reorientation transition to in-plane anisotropy occurs. Figure 4a depicts the switching field simulated for wires with tip-opening angles θ between 10◦ and 175◦. For a homogeneous anisotropy constant ($a = 1.0$, black squares), the geometry does not influence the switching field. Besides a reduction of the switching field, the same behavior is found for lower values of a homogeneous anisotropy constant down to $0.8\,K_1$ (not shown). This demonstrates that the reduction of the nucleation field reported above cannot be explained via the different opening angles of the tips. If we assume that the anisotropy constant is locally reduced in the range of the tips, we obtain a reduction of the switching field with decreasing tip-opening angle θ. This dependence is most pronounced for the highest reduction of $K'$. It is thus the amount of material with reduced anisotropy that determines the switching field. For an angle $\theta = 10°$, the maximum value of the switching field (that is $H_{max} = 415\,mT$ for flat wire ends) is reduced by 12%, 29%, 48%, and 67% for anisotropy reductions of 5%, 10%, 15%, and 20%, respectively. The simulated curves vary not only in the absolute reduction of the switching fields but also in the critical tip-opening angle at which the reduction sets in. While for $a = 0.95$ the switching field stays constant down to $\theta = 130°$, it drops below the maximum value already at $\theta = 155°$ for $a = 0.9$. The experimental values depicted in Fig. 3b stay constant for large angles as well and start to decrease somewhere between $\theta = 85°$ and $\theta = 75°$. While this behavior corresponds to a reduction of the local anisotropy constant at the wire end of less than 5%, the relative decrease of the nucleation field in our sample rather implies a reduction of about 18%.

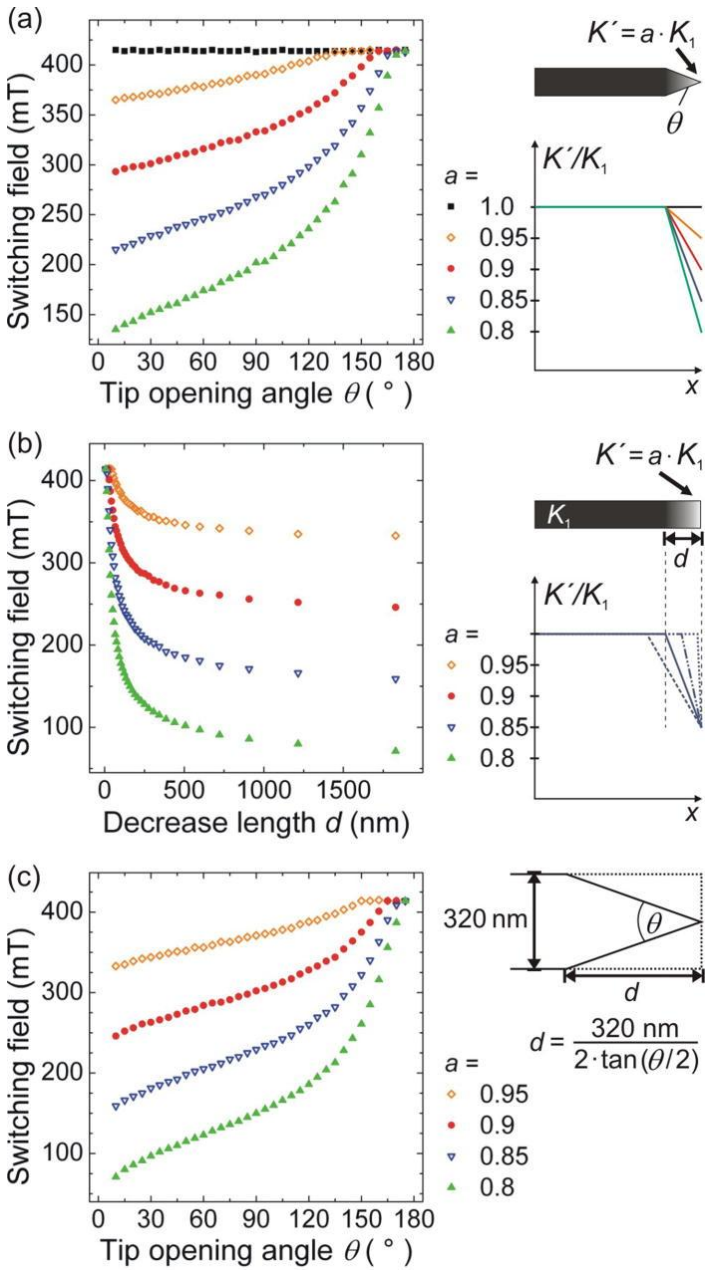


FIG.4

(a) Dependences of the switching field on the opening angle θ of the tip simulated for a wire with homogeneous anisotropy (black squares) as well as for wires with a linear reduction of the local anisotropy constant in the tip area from $K_1$ to $K' = a \cdot K_1$ (other color) as sketched on the right hand side. (b) Dependence of the switching fields on the total reduction of the anisotropy constant $K'$ along the decrease length $d$ simulated for rectangular-shaped wires. (c) Same data as in (b) plotted versus tip-opening angle θ that corresponds to a certain decrease length $d$ as illustrated on the right hand side.

The experimental data show a nearly perfect linear dependence on the tip-opening angle θ up to 90◦ in accordance with the simulations. For higher angles, the experimental nucleation field remains constant, while a strengthened increase is found in the simulations. A possible explanation for this discrepancy is that shadowing effects during sputter deposition lead to a continuous reduction of the film thickness at all edges of the wires, while in the simulation abrupt edges are assumed. The gradual decay of the film

thickness at the wire edges means that there is a gradual reduction of the anisotropy constant for all wires independent of the tip-opening angle. At sharp tips, the regions of both edges where the anisotropy decreases can overlap causing an anisotropy reduction in the whole tip area. For blunt tips, this effect is strongly reduced and the influence on the switching field is fading away. The experimental results therefore indicate that the reduction of the anisotropy constant is localized at the edges in contrast to the simulations where the anisotropy is taken as reduced in the whole tip region. This probably leads to a "saturation" of the increase of the nucleation field at $\theta \approx 90°$ in the experiment, since the gradual reduction of the film thickness at all edges has the same effect as the gradual reduction of the film thickness in the triangular-pointed ends when the tip-opening angle exceeds a critical value.

To further investigate the influence of the wire's geometry on the nucleation field, additional simulations have been performed. Instead of having one triangular-pointed end, nanowires were designed with two flat ends. Nevertheless, the anisotropy constant was reduced linearly at one end of the wire. Thereby the distance *d* over which the anisotropy decreases, corresponds to the length of a tip with a certain opening angle as sketched on the right hand side of Fig. 4c. Figures 4b,4c reveal that the switching fields show the same dependences but are stronger reduced in comparison to the switching fields of nanowires with triangular-pointed ends (compare Fig. 4a). This finding qualitatively shows that nucleation depends on the total area with reduced anisotropy constant, as in nanowires with flat ends this area is much larger than in nanowires with triangular-pointed ends. In particular, the region at the wire end, where the anisotropy constant is lowest, is significantly reduced in nanowires with triangular-pointed ends, compare sketch in Fig. 4c. Rectangular wires with a comparable linear reduction of the local anisotropy constant over the same decrease length *d* (and the corresponding tip-opening angle θ) thus provide a larger area for a certain nucleation volume to reverse and consequently have lower switching fields. With the same arguments, it can be explained why the switching field depends on the opening angle θ in wires with triangular-pointed ends: the smaller θ, the larger is the tip area available for nucleation.

## CONCLUSION

We have shown that the critical field for the nucleation and injection of domain walls in Co/Pt nanowires can be tuned and reduced by up to about 60% compared to the switching field of rectangular-shaped wires by designing triangularly pointed wire ends. The reasoning is based on the reduction of the perpendicular magnetic anisotropy within the tip region that is caused by shadowing effects during sputter deposition of the multilayer. As confirmed by micromagnetic simulations the reduction of the local anisotropy constant accompanied by an increase of the nucleation area in sharper tips accounts for the effect observed. A low nucleation field is a necessary prerequisite for the preparation of domain walls at comparably weak pinning sites as it is of interest for fundamental studies and applications.

## ACKNOWLEDGMENTS

The authors gratefully acknowledge financial support by the Deutsche Forschungsgemeinschaft via the Graduiertenkolleg 1286 and the Sonderforschungsbereich 668. The operation of the x-ray microscope is supported by the Director, Office of Science, Office of Basic Energy Sciences, of the U.S. Department of Energy under Contract No. DE-AC02-05-CH11231.

1. P. S. Ho and T. Kwok, Rep. Prog. Phys. **52**, 301 (1989).
2. O. Boulle, G. Malinowski, and M. Kläui, Mater. Sci. Eng. R **72**, 159 (2011).
3. G. Tatara and H. Kohno, Phys. Rev. Lett. **92**, 086601 (2004).
4. J. Xiao, A. Zangwill, and M. D. Stiles, Phys. Rev. B **73**, 054428 (2006).
5. P. Gambardella and I. M. Miron, Philos. Trans. R. Soc. London, Ser. A **369**, 3175 (2011).

6. P. P. J. Haazen, E. Murè, J. H. Franken, R. Lavrijsen, H. J. M. Swagten, and B. Koopmans, Nature Mater. **12**, 299, (2013).
7. M. Hayashi, L. Thomas, C. Rettner, R. Moriya, X. Jiang, and S. S. P. Parkin, Phys. Rev. Lett. **97**, 207205 (2006). [MEDLINE]
8. S. Hankemeier, A. Kobs, R. Frömter, and H. P. Oepen, Phys. Rev. B **82**, 064414 (2010).
9. S. S. P. Parkin, M. Hayashi, and L. Thomas, Science **320**, 190 (2008).
10. O. Boulle, J. Kimling, P. Warnicke, M. Kläui, U. Rüdiger, G. Malinowski, H. J. M. Swagten, B. Koopmans, C. Ulysse, and G. Faini, Phys. Rev. Lett. **101**, 216601 (2008).
11. L. S. E. Alvarez, K. Y. Wang, S. Lepadatu, S. Landi, S. J. Bending, and C. H. Marrows, Phys. Rev. Lett. **104**, 137205 (2010).
12. M. Cormier, A. Mougin, J. Ferré, A. Thiaville, N. Charpentier, F. Piechon, R. Weil, V. Baltz, and B. Rodmacq, Phys. Rev. B **81**, 024407 (2010).
13. C. Hassel, M. Brands, F. Y. Lo, A. D. Wieck, and G. Dumpich, Phys. Rev. Lett. **97**, 226805 (2006).
14. A. Aziz, S. J. Bending, H. G. Roberts, S. Crampin, P. J. Heard, and C. H. Marrows, Phys. Rev. Lett. **97**, 206602 (2006).
15. J. H. Franken, M. Hoeijmakers, H. J. M. Swagten, and B. Koopmans, Phys. Rev. Lett. **108**, 037205 (2012).
16. A. Kobs, S. Hesse, W. Kreuzpaintner, G. Winkler, D. Lott, P. Weinberger, A. Schreyer, and H. P. Oepen, Phys. Rev. Lett. **106**, 217207 (2011).
17. A. Kobs, S. Hesse, H. P. Oepen, and P. Weinberger, Philos. Mag. **92**, 2835 (2012).
18. J.-C. Lee, C.-H. Hsieh, C.-C. Chang, L.-W. Huang, L.-K. Lin, and S.-F. Lee, J. Appl. Phys. **113**, 17C714 (2013).
19. R. P. Cowburn, D. A. Allwood, G. Xiong, and M. D. Cooke, J. Appl. Phys. **91**, 6949 (2002).
20. M.-Y. Im, L. Bocklage, P. Fischer, and G. Meier, Phys. Rev. Lett. **102**, 147204 (2009).
21. A. Vogel, S. Wintz, J. Kimling, M. Bolte, T. Strache, M. Fritzsche, M.-Y. Im, P. Fischer, G. Meier, and J. Fassbender, IEEE Trans. Magn. **46**, 1708 (2010).
22. K. J. Kirk, J. N. Chapman, and C. D. W. Wilkinson, Appl. Phys. Lett. **71**, 539 (1997).
23. T. Schrefl, J. Fidler, K. J. Kirk, and J. N. Chapman, J. Magn. Magn. Mater. **175**, 193 (1997).
24. N. Bardou, B. Bartenlian, C. Chappert, R. Mégy, P. Veillet, J. P. Renard, F. Rousseaux, M. F. Ravet, J. P. Jamet, and P. Meyer, J. Appl. Phys. **79**, 5848 (1996).
25. F. Fournel, Y. Chen, F. Carcenac, N. Essaidi, H. Launois, V. Kottler, and C. Chappert, IEEE Trans. Magn. **34**, 1027 (1998).
26. T. Ono, H. Miyajima, K. Shigeto, K. Mibu, N. Hosoito, and T. Shinjo, J. Appl. Phys. **85**, 6181 (1999).
27. J. Fassbender, D. Ravelosona, and Y. Samson, J. Phys. D: Appl. Phys. **37**, R179 (2004).
28. L. S. E. Alvarez, G. Burnell, C. H. Marrows, K.-Y. Wang, A. M. Blackburn, and D. A. Williams, J. Appl. Phys. **101**, 09F508 (2007).
29. D. Chiba, G. Yamada, T. Koyama, K. Ueda, H. Tanigawa, S. Fukami, T. Suzuki, N. Ohshima, N. Ishiwata, Y. Nakatani, and T. Ono, Appl. Phys. Express **3**, 073004 (2010).
30. Silicon-nitride membranes were purchased from Silson Ltd., UK.
31. As resist PMMA A4 from MicroChem was used.
32. H. Stillrich, C. Menk, R. Frömter, and H. P. Oepen, J. Appl. Phys. **105**, 07C308 (2009).
33. . Fischer, Mater. Today **13**, 14 (2010).
34. C. T. Chen, F. Sette, Y. Ma, and S. Modesti, Phys. Rev. B **42**, 7262 (1990).
35. See http://micromagnum.informatik.uni-hamburg.de; The simulation parameters are $K_1$=1.58×10$^6$ J/m$^3$, $M_s$=1.4×10$^6$ A/m, and exchange constant $A$=30×10$^{-12}$ J/m. The magnetic anisotropy $K_1$ of the Co/Pt multilayer was determined experimentally from a hard-axis remagnetization curve probed with magneto-optical Kerr-effect[32] using $K_{1,\mathrm{eff}}$=(350±30)

kJ/m$^3$=$K_1$−$\frac{\mu_0 M_s^2}{2}$. A high Gilbert damping parameter of $\alpha$=0.1 was chosen in order to avoid unrealistic dynamic effects as the field in the experiment is reduced slowly compared to the micromagnetic time-scale.
36. H. Kronmüller, Phys. Status Solidi B **144**, 385 (1987
37. H. Kronmüller and S. S. P. Parkin, *Handbook of Magnetism and Advanced Magnetic Materials* (John Wiley & Sons, 2007).
38. Z. S. Shan, J. X. Shen, R. D. Kirby, D. J. Sellmyr, and Y. J. Wang, J. Appl. Phys. **75**, 6418 (1994).
39. G. Schütz, R. Wienke, W. Wilhelm, W. B. Zeper, H. Ebert, and K. Spörl, J. Appl. Phys. **67**, 4456 (1990).
40. T. Gerhardt, A. Drews, and G. Meier, J. Phys.: Condens. Matter **24**, 024208 (2012).
41. H. Stillrich, C. Menk, R. Frömter, and H. P. Oepen, J. Magn. Magn. Mater. **322**, 1353 (2010).
42. W. B. Zeper, F. J. A. M. Greidanus, P. F. Carcia, and C. R. Fincher, J. Appl. Phys. **65**, 4971 (1989).
43. M. Kisielewski, A. Maziewski, M. Tekielak, J. Ferré, S. Lemerle, V. Mathet, and C. Chappert, J. Magn. Magn. Mater. **260**, 231 (2003).
44. C.-J. Lin, G. L. Gorman, C. H. Lee, R. F. C. Farrow, E. E. Marinero, H. V. Do, H. Notarys, and C. J. Chien, J. Magn. Magn. Mater. **93**, 194 (1991).
45. R. L. Stamps, L. Louail, M. Hehn, M. Gester, and K. Ounadjela, J. Appl. Phys. **81**, 4751 (1997).
46. T. Thomson, G. Hu, and B. D. Terris, Phys. Rev. Lett. **96**, 257204 (2006).
47. J. W. Lau, R. D. McMichael, S. H. Chung, J. O. Rantschler, V. Parekh, and D. Litvinov, Appl. Phys. Lett. **92**, 012506 (2008).
48. J. M. Shaw, S. E. Russek, T. Thomson, M. J. Donahue, B. D. Terris, O. Hellwig, E. Dobisz, and M. L. Schneider, Phys. Rev. B **78**, 024414 (2008).

## DISCLAIMER